Journal Pre-proof

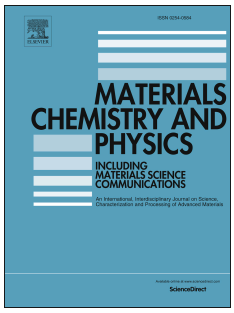

Development of thickness-tunable gold nanorods for anti-oxidant detection

Debolina Chakraborty, Megala Venkatesan, K.R. Ethiraj, N. Chandrasekaran, Amitava Mukherjee

PII: S0254-0584(19)31110-1

DOI: https://doi.org/10.1016/j.matchemphys.2019.122295

Reference: MAC 122295

To appear in: *Materials Chemistry and Physics*

Received Date: 12 July 2019

Revised Date: 4 October 2019

Accepted Date: 9 October 2019

Please cite this article as: D. Chakraborty, M. Venkatesan, K.R. Ethiraj, N. Chandrasekaran, A. Mukherjee, Development of thickness-tunable gold nanorods for anti-oxidant detection, *Materials Chemistry and Physics* (2019), doi: https://doi.org/10.1016/j.matchemphys.2019.122295.

Development of thickness-tunable gold nanorods for anti-oxidant detection

Debolina Chakraborty[2], Megala Venkatesan[1], K.R. Ethiraj[2], N. Chandrasekaran[1], Amitava Mukherjee[1]*

[1] Centre for Nanobiotechnology, Vellore Institute of Technology, Vellore, India.

[2] School of Advanced Science, Vellore Institute of Technology, Vellore, India.

***Corresponding author**

Dr. Amitava Mukherjee
Senior Professor & Deputy Director
Centre for Nanobiotechnology
Vellore Institute of Technology, Vellore – 632014, India.
Email: amit.mookerjea@gmail.com, amitav@vit.ac.in
Phone: 91 416 2202620
Fax: 91-416-224309

Abstract

Here, in this study, we strategically utilized low- energy mediated epitaxial deposition of Au^0 atoms reduced by gallic acid over preformed gold nanorods (GNRs) seeds. It can be suggested that GNRs seed/Au^{3+} ratio influences the directional attachment of Au^0 atoms to the GNRs. Alteration in the thickness of the GNRs upon deposition of Au^0 in presence micromolar levels of antioxidant reduces the aspect ratio of the nanorods. Change in the aspect ratio altogether induces a blue-shift in the longitudinal surface plasmon resonance (LSPR) of the GNRs from the NIR region of the spectrum to the shorter wavelength. TEM imaging, DLS and zeta potential analyses confirms the morphological and surface-charge alterations after interaction with antioxidant. Based on the relation between blue-shift of the LSPR band and the concentration of gallic acid, the sensing platform achieves a linear detectable range of 1.25-35 µM with detection limit as low as 90 nM and the limit of quantification as 300 nM. The method has high selectivity against tested interferents and was found to be reproducible. The potential application of the developed sensor was validated by quantifying gallic acid in commercially available apple juice. High recovery (99.46-100.4 %) was obtained, suggesting that the established assay which is reliable and facile can be successfully used for gallic acid detection real food samples. The developed method of tuning the aspect ratio of nanomaterial can be further extended for detection other anti-oxidant molecules.

Keywords: Gallic acid; Gold nanorods; Seed-mediated growth; Surface plasmon resonance;

1. Introduction

Over the past few decades, metal nanoparticles (NPs) such as gold and silver NPs have gained immense recognition in nanosensing, therapeutics, and diagnostic applications.[1, 2] In this regard, ease of synthesis, versatile surface functionalization and long term stability of gold nanomaterials increases their potential as efficient detection probes.[3] Their tunable optical property due to surface plasmon resonance (SPR) makes them ideal for sensing several environmental as well as biological analytes.[4] Several recent reports have shown gold NPs based disease diagnosis wherein different principles such as SERS, modified SPR, altered dynamic light scattering, and colorimetry has been utilized.[5] Further enzyme detection depending on the size of gold NPs have also been reported. In another important study, Dondapati et al. have demonstrated the use of biotin-modified gold nanostars for sensing streptavidin.[6] Sensing applications using other shapes of gold nanomaterials include the use of gold nanowires and nanocubes for detection of bacteria in human kidney infection and catechol, respectively.[7, 8]

The plasmon resonance of (GNRs) is highly dependent on its size and shape.[9] The two plasmonic peaks representing the width and length of GNRs are denoted as TSPR and LSPR, where TSPR is generally ~ 500 nm, and the LSPR can be tuned anywhere within the visible to the near-IR region of the spectra (600 – 1100 nm). This flexible LSPR of GNRs make them suitable for several photothermal, biomedical imaging and sensing applications [10]. Apart from these, the properties of the LSPR can be utilized for plasmon-accelerated electrochemical reactions, electrocatalysis, detection and imaging of telomerase activity, cellular alkaline phosphatase activity and circulating cancer cells (CTCs) [11-15].The LSPR is reported to be highly sensitive to the change in the refractive index of the medium. The spectral shift thus can be utilized for sensing minor changes in the solvents.[16] Morphological modifications in terms of changing the aspect ratio (AR) or shape of gold nanorods (GNRs) in the presence of foreign analytes has also been reported to effective in inducing significant red and blue shift in the LSPR.[17] Such variations can be monitored for efficient sensing of molecules and improving the limit of detection (LOD). Further, Parab et al. have also employed GNRs as a SERS substrate wherein they have achieved highly sensitive and selective detection of DNA.[18] In other words,

several analytical protocols based on tuning of LSPR can be developed to sensitive, selective and precise detection of chemical and biological molecules.

Several NPs-based gallic acid detection methods have already been reported [19, 20]. SiO_2 nanoparticles on modified carbon paste electrode, Fe_2O_3/electro-reduced graphene oxide composite and polyepinephrin/ glassy carbon electrode have been employed previously for gallic acid detection [21-23]. Though the developed methods enhance the sensitivity but intricate fabrication of such electrode- based sensing platforms remains a challenging concern.

The current study, aimed at fabricating a sensitive and facile sensing platform that has a wide detection range, minimal instrumentation cost as well as requires less detection time. The sensing strategy is based on the hypothesis that the presence of phenolic compound such as gallic acid would facilitate the reduction of Au^{3+} to Au^0. The reduced Au atoms would coat the native surface of GNRs via heterogeneous nucleation considering the thermodynamically favourable condition. It can be suggested that in a typical seed-mediated process, the seed /Au^{3+} ratio influences the deposition of reduced Au in a controlled-direction, generating shorter rods and few spheres. As a consequence of the formation of the Au layer, the thickness of the GNRs increases, therefore, reducing its aspect ratio (Scheme 1). To the best of our knowledge, this is the first-ever work that utilizes the strategy of altering the aspect ratio of GNRs by tuning its breadth in the presence of an anti-oxidant. The described strategy overcomes several limitations associated with previously developed methods that are time-consuming, employs fabrication of complex composites and also requires high-end instruments along with trained personnel. Not only the technique developed is reliable, simple, and reproducible for detection of gallic acid but also opens scope for quantification of other vital anti-oxidants. Based on the proposed principle, the rod-shaped GNRs can be efficiently utilized to sense gallic acid in the range of 1.25-35 μM with a low detection limit of 90 nM. The developed nanosensing platform provides good selectivity as well as high recovery rates (99.4-103.4%) when used for quantifying gallic acid in real food samples.

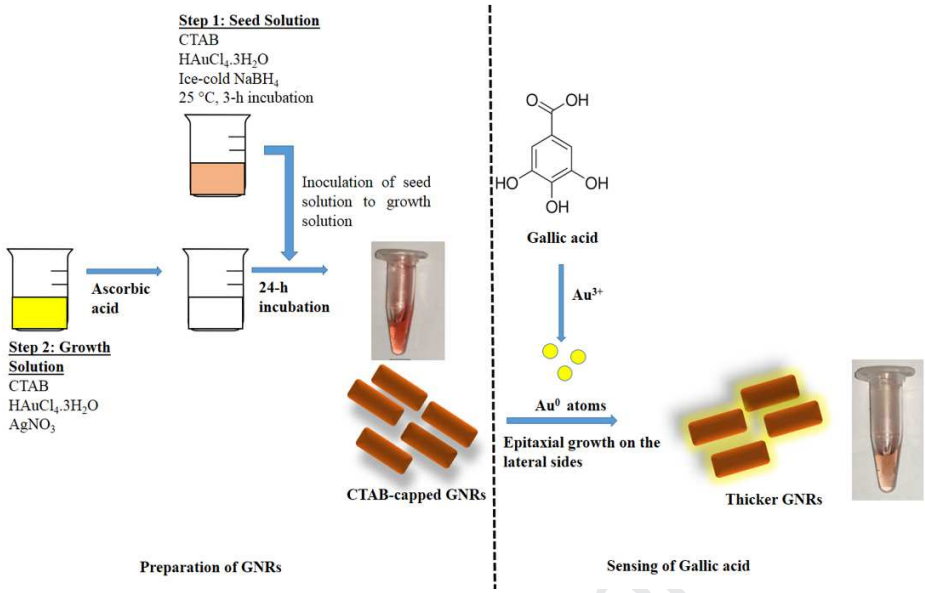

Scheme 1. Schematic presentation showing preparation of GNRs and strategic detection of gallic acid based on the deposition of Au^0 on the GNRs seeds.

2. Materials and Methods

2.1. Chemicals

Sodium borohydride ($NaBH_4$), Cetyltrimethylammonium bromide (CTAB), gallic acid were purchased from Sigma-Aldrich (India). Hydrogen tetrachloroaurate hydrate ($HAuCl_4.2H_2O$) and salts for the interference study, were purchased from SRL Pvt. Limited (India). Ascorbic acid and silver nitrate ($AgNO_3$) were obtained from MERCK (India) and SD Fine Chemicals (India), respectively. Antioxidant molecules such as cinnamic acid, alpha tocopherol and quercetin were procured from Qualigens Fine Chemicals Pvt. Limited and Sigma-Aldrich (India) respectively. Glucose, Na_3PO_4, L-arginine and L-cysteine were purchased from Himedia (India). For all the experiments, ultrapure deionized water (18.2 MΩ.cm) from Cascada Bio Water filtration unit (Pall Corporation, Ann Arbor, Michigan, USA) was used. All the glasswares used for the experiment were washed thoroughly in aqua regia, followed by rinsing with deionized water.

2.2. Synthesis of gold nanorods

Modified El-Sayed method was used for the synthesis of rod-shaped GNRs. Two separate solutions, namely seed solution and growth solutions, were prepared. The seed solution was

prepared as follows. Briefly, ice-cold $NaBH_4$ (0.3 mL, 0.01M) was added to solution mixture containing $HAuCl_4$ (0.5 mM) and CTAB (0.2 M) in a volume ratio of 1:1. The entire reaction mixture was incubated at room temperature for 3 h. For the growth solution, a 200 mL solution containing $HAuCl_4$ (0.5 mM) and CTAB (0.1 M) was made and to this 6 mL of $AgNO_3$ (4 mM) was added. Following this 0.5 M of H_2SO_4 (1 mL) and 0.0788 M ascorbic acid (1.4 mL) were further added and mixed gently. For the final step, the pre-prepared seed solution (0.24 mL) was added to the above growth solution mixture and left at room temperature for a period of 12 h. The brownish coloured solution was centrifuged 9000 rpm (2 times) for 30 min to remove the unbound CTAB and stored at room temperature (28 °C). [24]

2.3. Evaluating gallic acid concentration using gold nanorods

Gallic acid was used as the reducing agent for the reduction of $HAuCl_4$. Stock gallic acid was made freshly in deionized water before the start of the experiment. Stock gallic acid was serial diluted and 160 µL of gallic acid with appropriate concentration was added to a solution mixture containing 320 µL GNRs, 160 µL $HAuCl_4$ and 160 µL phosphate buffer (pH- 7.4). The mixture was incubated for 30 min following which UV-spectral, dynamic light scattering and zeta-potential and TEM analysis.

2.4. Selectivity of gallic acid detection

For assessing, the selectivity of the GNR-based detection probe, 0.3 mM of interferents such as NaCl, KCl, ZnSO4, $CuSO_4$, $FeCl_3$, Glucose, Na_3PO_4, ascorbic acid, L-arginine and L-cysteine were added instead of gallic acid. The standard assay, as mentioned above in section 2.3, was followed systematically.

2.5. Estimation of gallic acid in apple juice

Commercially available apple juice was pre-treated before utilizing its gallic acid detection. Briefly, the procured juice was centrifuged at 10000 rpm for 5 min. The supernatant obtained was filtered and diluted with deionized water to obtain an appropriate concentration for assay. Briefly, 160 µL of pre-treated apple juice sample with was added to a solution mixture containing 320 µL GNRs, 160 µL $HAuCl_4$ and 160 µL phosphate buffer. The solution mixture was allowed to stand at room temperature for 30 min, following which UV-spectroscopic measurements were taken.

2.6. Instrumentation

For characterizing CTAB-capped GNRs high-resolution transmission electron microscopy (HR-TEM) (JEOL JEM 2100, Japan) was used. The operating voltage was 200 kV. As synthesized GNRs were sonicated for 10 min before coating on carbon-coated copper grids. Analysis of the working concentration of GNRs was done using ICP-OES (Perkin Elmer Optima 5300DV, USA), the wavelength for the measurement was 267.595. For spectral analysis, UV-Visible spectrophotometer (Evolution 220, Thermo Scientific) was used in the wavelength range of 200-900 nm. The MHD and surface charge of the CTAB-capped GNRs before and after the interaction was measured using 90 Plus Particle Analyzer (Brookhaven Instruments Corporation, USA).

3. Results and discussion

3.1. Characterization of gold nanorods

Fig. 1 shows the rod-shaped morphology of as-synthesized CTAB GNRs. The NRs were monodisperse, with an average aspect ratio of 2.89. The length and breadth of the GNRs were calculated to be 63.01 ± 1.87 and 21.76 ± 0.78 nm, respectively (Particle count -200). Fig. 2 shows the SAED pattern of CTAB-capped GNRs, the obtained d-spacing values 0.094, 0.239, 0.148 nm, corresponds to (420), (111) and (220) spacing of fcc Au.[25] The concentration of the as synthesized GNRs was 152.6 µM as estimated by ICP-OES. Fig. S1 shows the UV- spectral analysis of as-synthesized CTAB- GNRs. The GNRs had two absorption peaks representing the LSPR at 802 nm and TSPR at 515 nm. The mean hydrodynamic diameter of the NRs was observed to be 80.3 ± 1.3 nm and the surface charge of +42.3 ± 0.75 mV.

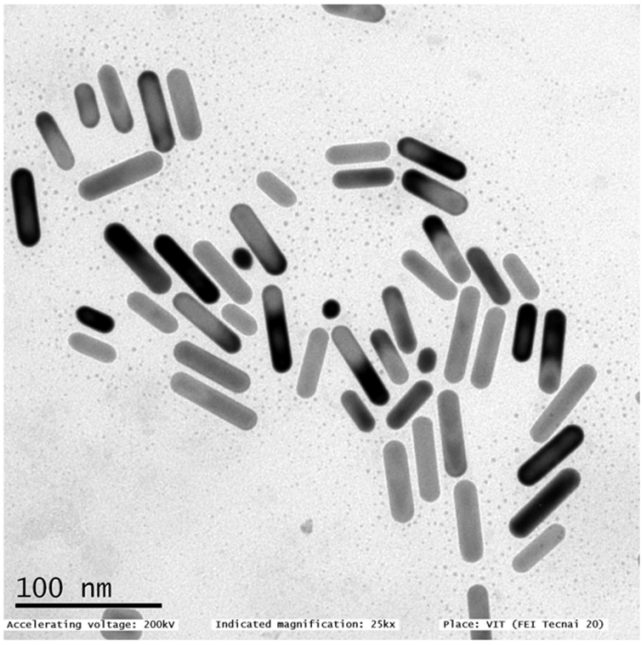

Fig. 1. TEM image of as synthesized CTAB-capped GNRs

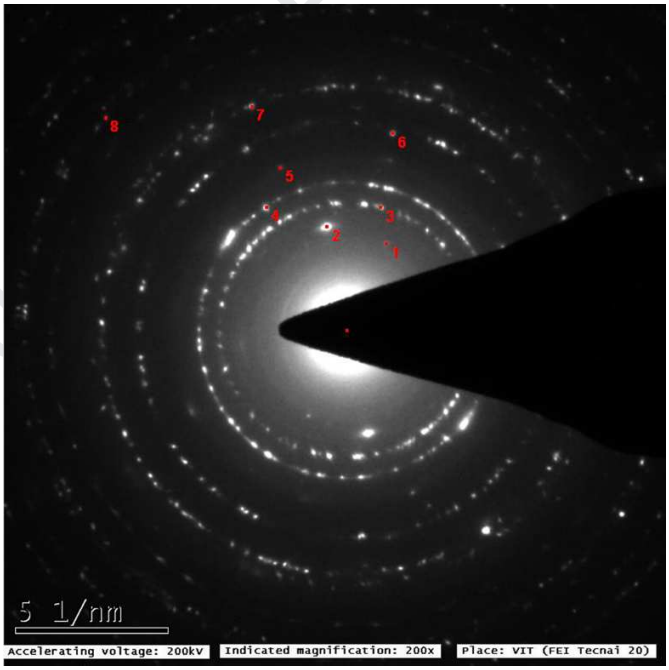

Fig. 2. SAED pattern of as synthesized CTAB-capped GNRs

3.2. Optimization of reaction parameters

Alteration in the thickness and overall morphology of the GNRs in the presence of gallic acid was investigated under optimized conditions. Reports suggest that GNRs have limited

stability beyond pH-7, leading to particle aggregation and disappearance of the LSPR. Even gallic acid loses its inherent stability at high pH. Hence considering stability of both seed and reducing agent as important criteria for seed-mediated growth a neutral pH of 7.4 was chosen for the experiments [26, 27]. Primary parameters such as the optimum concentration of growth precursor and time were investigated systematically. Briefly, different concentrations of $HAuCl_4.3H_2O$ in the range 0.5-4 µM was interacted with the GNRs in the presence and absence of gallic acid. Fig. 3 (A) shows that, in the absence of reducing agent, λmax of the GNRs almost remained constant. However, in the presence of gallic acid, the maximum blue-shift (~781 nm) was observed for 2.5 µM concentration of the Au^{3+}. Addition of higher concentration of precursor did not induce any significant change in the LSPR. It can be suggested that the introduction of higher concentrations of growth precursor (beyond 2.5 µM) causes saturation of Au^{3+} in the medium, thus promoting the formation of small spheres via homogeneous nucleation.[28] The response generated over a period of time was studied, and it was observed that for control samples (without gallic acid), the λmax remained constant at ~ 807 nm. However, in the presence of gallic acid, the LSPR blue-shifted to ~779 nm for an incubation period of 30 min (Fig. 3(B)). No significant change in the λmax was observed after 30 min. Hence for further studies the response time for the gallic acid nanosensor was taken as 30 min.

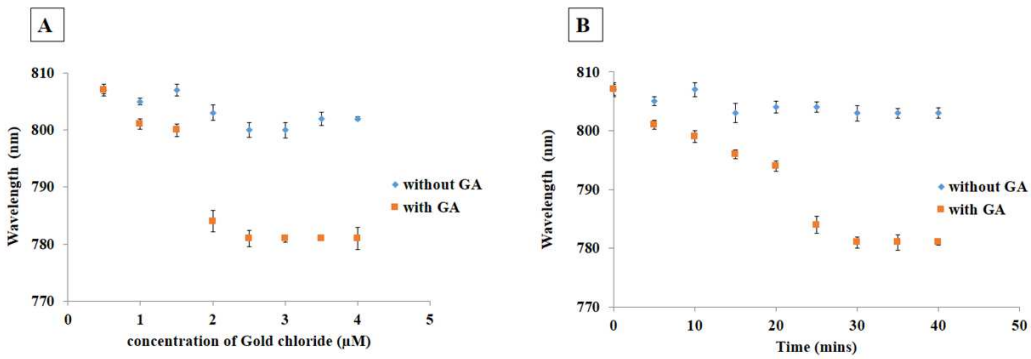

Fig. 3. Analyses of change in LSPR of GNRs after interaction with and without gallic acid (A) in presence of different concentration of HAuCl4. $3H_2O$ (B) at different time point

3.3. Development of bilayered GNR using gallic acid

The LSPR of GNRs is sensitive to the changes in the aspect ratio. Herein, under the optimized condition, the aspect ratio of the as-synthesized GNRs was modified in a controlled fashion. Upon introduction of Hydrogen tetrachloroaurate hydrate and gallic acid as growth

precursor and reductant, respectively, the Au^{3+} converts to Au^0. [29] Employing GNRs as seeds, the reduced atoms undergoes seed-mediated growth through thermodynamically favourable heterogeneous nucleation and not homogeneous nucleation.[30] It can be said that, in the presence of an excess amount of GNRs seed, there is increased competition between available seed particles and the Au^{3+} ions. As a consequence of the shortage of Au^{3+} ions per seed particle, the elongation of GNRs at the tip is retarded.[31] Considering the NRs AR (length to breadth ratio), seed-mediated epitaxial deposition of Au^0 was seen to increase the thickness of GNRs, altogether reducing its aspect ratio (Scheme 2). Parameters such as shape, size and composition of the metal NPs determine the LSPR properties of nanocrystals.[32, 33] NRs with higher AR is said to have absorption spectra near the NIR region, whereas the ones with smaller AR have LSPR towards the shorter wavelength.[34] Fig. 4 (A) and (B) demonstrates the GNRs with an average AR of 2.38 and 2.01 after interaction with $HAuCl_4$ in the presence of 15 and 30 µM of gallic acid, respectively. The LSPR blue shifted from 805 nm to 714 nm. An increase in the intensity of the LSPR of the interacted NRs also indicates that microlevel concentration of gallic acid can efficiently promote seed-mediated Au^0 deposition on the GNRs (Fig. 5). Similar reports have been shown previously wherein, in the presence of anti-oxidants deposition of Ag^0 on GNRs induced blue shift in the LSPR along with an increase in absorption intensity. The mean hydrodynamic diameter (MHD) of the 30 µM gallic acid interacted NRs were seen to increase to 86.3± 2.6. As that for zeta-potential, deposition of newly formed Au^0 slightly reduced surface-charge of the native GNRs from +42.12 to +37.82 mV. Table 2 summarizes the changes in the GNRs before and after interaction with $HAuCl_4$ and gallic acid.

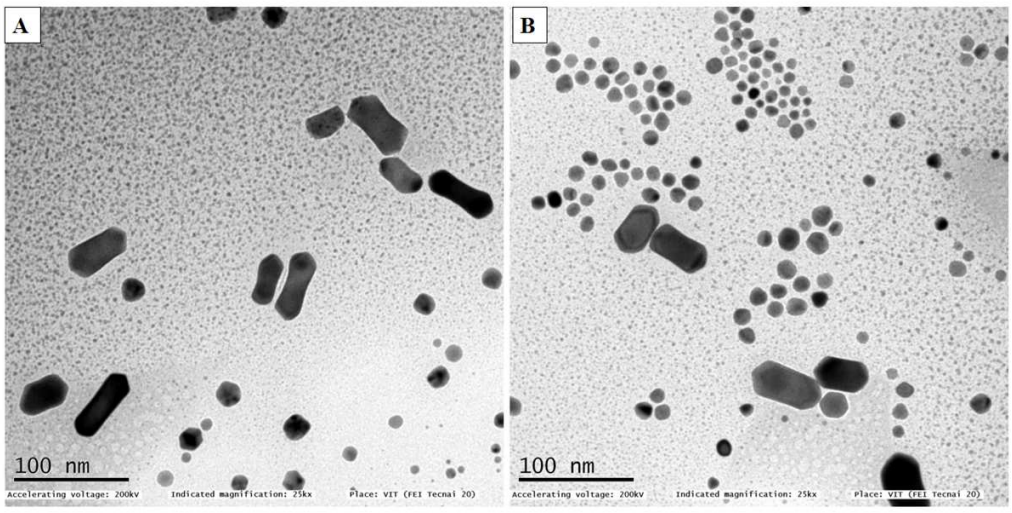

Fig. 4 TEM image of CTAB-capped GNRs after interaction with HAuCl4. $3H_2O$ (2.5 μM) in presence of (A) 15 μM (B) 30 μM of gallic acid

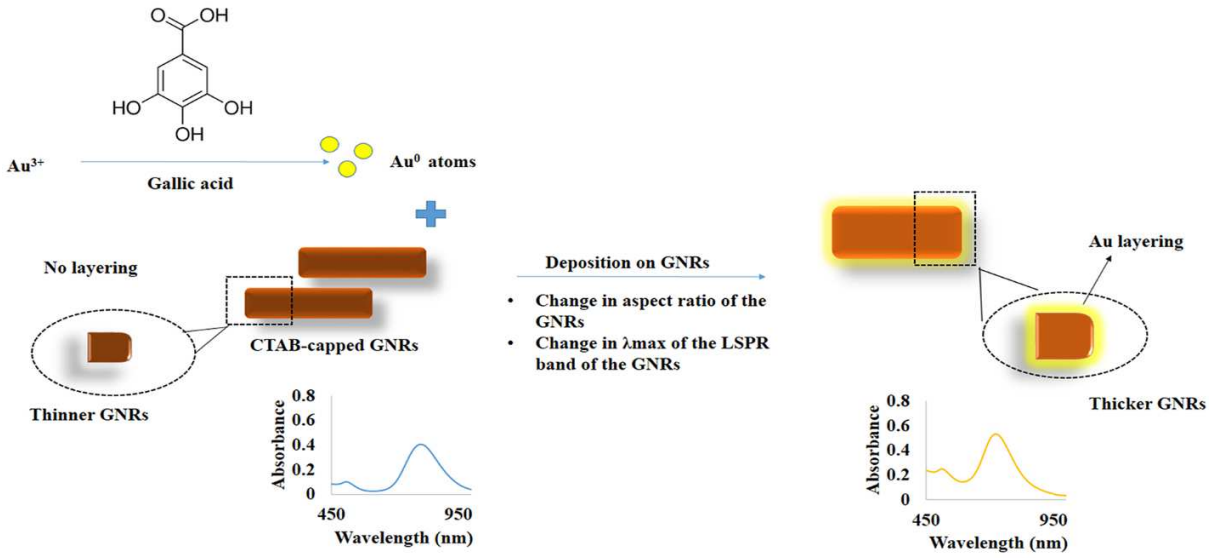

Scheme 2. Schematic presentation showing change in the morphology of the GNRs and their LSPR band in presence of gold chloride and gallic acid.

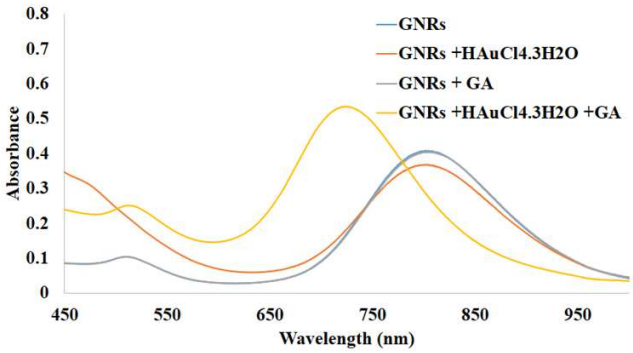

Fig. 5. UV-Visible spectrum of as such CTAB-capped GNRs and after interaction with $HAuCl_4$. $3H_2O$ (2.5 μM); after interaction with gallic acid (35 μM); after interaction with $HAuCl_4$. $3H_2O$ (2.5 μM) and gallic acid (35 μM)

3.4. Sensitivity and precision analysis of the bilayered GNRs probe

The concept of tuning the AR of the GNRs in the presence of anti-oxidant can be carefully controlled under optimized conditions for quantitative detection of gallic acid. Fig. 6 shows the normalized extinction spectra wherein, in the presence of a growth precursor, a

constant hypsochromic shift in the LSPR band of the GNRs can be seen with increasing concentrations of gallic acid (1.25, 2.5, 5, 10, 15, 20, 25, 30, 35 µM). It can be noted that the dark brownish colour of the as synthesized CTAB-capped GNRs changed to light brown following addition of 35 µM of gallic acid. The GNRs solution mixture appeared light pinkish and yellowish upon addition of 15 and 1.25 µM of gallic acid respectively (Fig. S2). However, concentrations beyond 30 µM did not induce any significant shift of the LSPR (Fig. S3). The standard calibration curve for gallic acid concentration vs change in the LSPR peak (Δλ) was plotted, and a good linear correlation (R^2= 0.9922) was obtained (Fig. 7). For the gallic acid concentration range of 1.25-35 µM, the linear regression equation was established to be y = 2.6279x + 1.9159. The LOD and LOQ were calculated by measuring the spectral scan of the blank GNRs (n=5). The mean and standard deviation (SD) of the λmax of the LSPR was found to be 805 ± 0.08. The experimentally calculated LOD using the equation (3*SD)/Slope of the linear regression line was 90 nM. The LOQ was calculated using the equation (10*SD)/Slope of the linear regression line and was found to be 300 nM. All the experiments were performed in triplicates (n=3). The response for different concentration of gallic acid was calculated using one –way ANOVA and was found to be statistically significant ($p<0.05$). A comparable sensitivity of the developed GNRs based gallic acid sensing platform with the previously reported state-of-the-art techniques has been summarized in table 2. It can be suggested that the GNRs-based nanosensor has high sensitivity along with a relatively wide linear range of detection. The working principle of the fabricated method is simple and also reduces the time and cost for high-end instrumentations required in other assays.

The reproducibility of the developed method was evaluated by analyzing run-to-run, day-to-day and batch-to-batch for different concentrations of gallic acid (Table S1). Relative standard deviation (% RSD) observed, i.e. 1.14, 1.18 and 2.32, respectively. Relatively low % RSD ascertains the reproducibility of the developed sensing system. The overall analytical performance of the nanosensor has been listed in table 3.

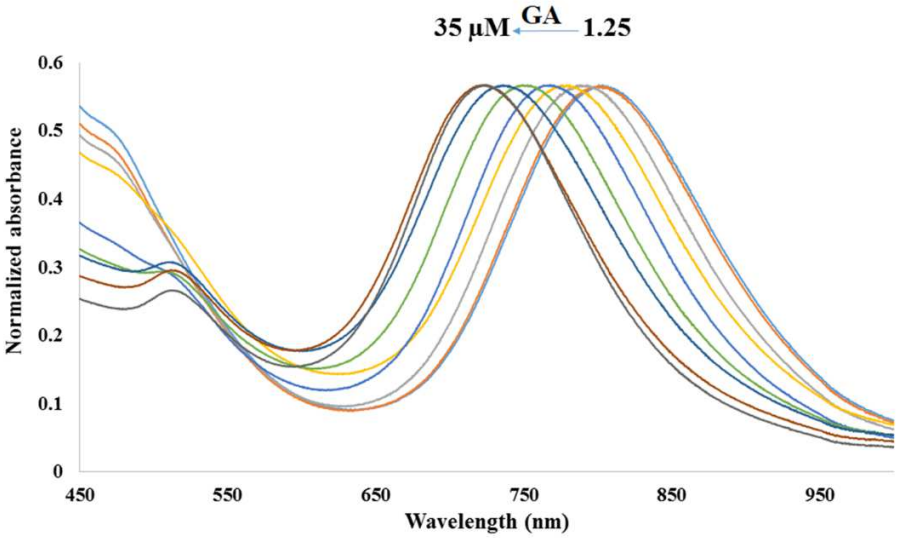

Fig. 6. Normalized UV-Visible absorption spectrum of GNRs showing blue-shift upon interaction with increasing concentration of gallic acid

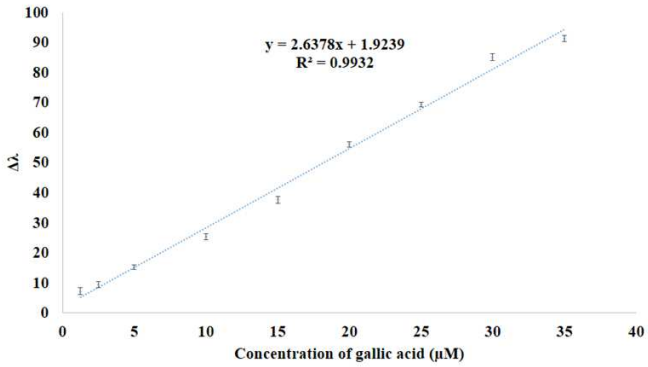

Fig. 7. Standard calibration curve for gallic acid concentration vs change in the LSPR peak (Δλ)

3.5. Studying the selectivity of the bilayered GNRs probe

The performance of the bilayered GNRs was assessed in the presence of other analytes that are commonly present in fruit juices. Fig. 8 represents the Δλ fluctuations observed when 100- fold excess (0.3 mM) of other interferents were introduced in the system. The spectral shift of the LSPR was highest for gallic acid, whereas for other interferents it was observed to be within 5%. However, for glucose and ascorbic acid, the Δλ fluctuation was seen to be slightly higher as compared to the other interferents (within 10 %). In the presence of other commonly reported antioxidants present in natural foods, such as cinnamic acid and quercetin, the Δλ

fluctuation was slightly higher. The generated response was similar to that observed for ascorbic acid. However, for Alpha tocopherol the Δλ fluctuation was within 5%. Considering the reducing nature of other antioxidants, it can be suggested that the developed assay can also be used for detecting similar analytes [35, 36]. Similar results were reported previously wherein, presence of growth precursor and potential anti-oxidant in the assay system were seen to induce a blue shift of the LSPR. [37]

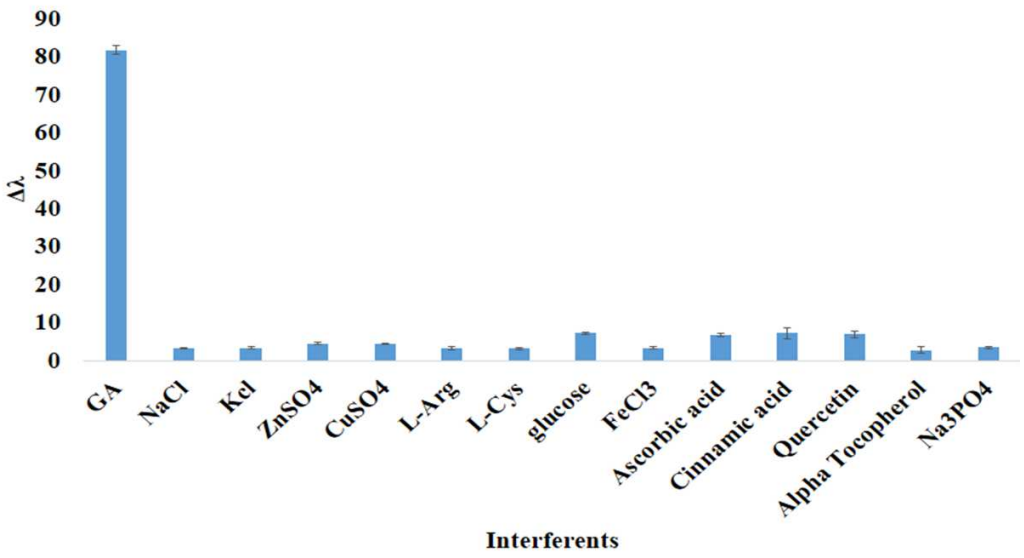

Fig. 8. Selectivity of the nanosensor in presence of interferents

3.6. Detection of gallic acid in apple juice

Application of the GNRs based nanosensor was tested by determining the gallic acid in commercially available apple juice. Standard addition method was followed wherein, standard gallic acid of 5, 10 and 20 µM was spiked into pre-treated juice sample. From the values depicted in table 4, it can be concluded that upon addition of different concentrations of gallic acid, the response obtained correlated well with the standard curve. The recovery % was seen to be 99.46, 100.46 and 103.4, respectively. The % RSD was within the acceptable range. The

observations suggest that developed nanosensing platform is reliable and can be practically applied for gallic acid detection in real samples.

4. Conclusion

In the current study, an analytical method based on thermodynamically favourable seed-mediated heterogeneous nucleation is applied to sense gallic acid. The redox reaction between the growth precursor and the gallic acid leads to deposition of the reduced Au atoms on preformed GNRs seeds. An overall morphological change in the GNRs after attachment of Au atoms modifies its aspect ratio and optical properties. The deposition causes blue-shift of the LSPR band. Several characterization TEM, DLS and zeta potential analyses indicates that the epitaxial growth induces a change in the aspect ratio and surface charge of the NRs. Under optimized conditions, the developed assay can be used to detect gallic acid in the linear range of 1.25- 35 µM. The LOD and LOQ were found to be 90 nM and 300 nM respectively. The nanosensor was highly reproducible and had excellent selectivity. The method showed good recovery (99.4-103 %) for commercially available apple juice. The nanosensing platform is reliable, facile, cost-effective and less labor intensive. It can be suggested, that the developed strategy under optimized conditions can be applied for sensing other essential anti-oxidants. Apart from this, the nanomaterial with aspect ratio tunable property can be possibly used for several biomedical applications.

References

[1] T.K. Sau, A.L. Rogach, F. Jäckel, T.A. Klar, J. Feldmann, Properties and applications of colloidal nonspherical noble metal nanoparticles, Advanced Materials 22(16) (2010) 1805-1825.
[2] G. Doria, J. Conde, B. Veigas, L. Giestas, C. Almeida, M. Assunção, J. Rosa, P.V. Baptista, Noble metal nanoparticles for biosensing applications, Sensors 12(2) (2012) 1657-1687.
[3] A.S. Emrani, N.M. Danesh, P. Lavaee, M. Ramezani, K. Abnous, S.M. Taghdisi, Colorimetric and fluorescence quenching aptasensors for detection of streptomycin in blood serum and milk based on double-stranded DNA and gold nanoparticles, Food chemistry 190 (2016) 115-121.
[4] K. Saha, S.S. Agasti, C. Kim, X. Li, V.M. Rotello, Gold nanoparticles in chemical and biological sensing, Chemical reviews 112(5) (2012) 2739-2779.
[5] L. Tong, H. Wei, S. Zhang, H. Xu, Recent advances in plasmonic sensors, Sensors 14(5) (2014) 7959-7973.
[6] S.K. Dondapati, T.K. Sau, C. Hrelescu, T.A. Klar, F.D. Stefani, J. Feldmann, Label-free biosensing based on single gold nanostars as plasmonic transducers, Acs Nano 4(11) (2010) 6318-6322.
[7] M. Basu, S. Seggerson, J. Henshaw, J. Jiang, R. del A Cordona, C. Lefave, P.J. Boyle, A. Miller, M. Pugia, S. Basu, Nano-biosensor development for bacterial detection during human kidney infection: use of glycoconjugate-specific antibody-bound gold NanoWire arrays (GNWA), Glycoconjugate Journal 21(8-9) (2004) 487-496.
[8] M.N. Karim, J.E. Lee, H.J. Lee, Amperometric detection of catechol using tyrosinase modified electrodes enhanced by the layer-by-layer assembly of gold nanocubes and polyelectrolytes, Biosensors and Bioelectronics 61 (2014) 147-151.
[9] M. Grzelczak, J. Pérez-Juste, P. Mulvaney, L.M. Liz-Marzán, Shape control in gold nanoparticle synthesis, Chemical Society Reviews 37(9) (2008) 1783-1791.
[10] L. Vigderman, B.P. Khanal, E.R. Zubarev, Functional gold nanorods: synthesis, self-assembly, and sensing applications, Advanced materials 24(36) (2012) 4811-4841.
[11] C. Wang, X.-G. Nie, Y. Shi, Y. Zhou, J.-J. Xu, X.-H. Xia, H.-Y. Chen, Direct plasmon-accelerated electrochemical reaction on gold nanoparticles, ACS nano 11(6) (2017) 5897-5905.
[12] Y. Shi, J. Wang, C. Wang, T.-T. Zhai, W.-J. Bao, J.-J. Xu, X.-H. Xia, H.-Y. Chen, Hot electron of Au nanorods activates the electrocatalysis of hydrogen evolution on MoS2 nanosheets, Journal of the American Chemical Society 137(23) (2015) 7365-7370.
[13] K. Wang, L. Shangguan, Y. Liu, L. Jiang, F. Zhang, Y. Wei, Y. Zhang, Z. Qi, K. Wang, S. Liu, In situ detection and imaging of telomerase activity in cancer cell lines via disassembly of plasmonic core–satellites nanostructured probe, Analytical chemistry 89(13) (2017) 7262-7268.
[14] K. Wang, L. Jiang, F. Zhang, Y. Wei, K. Wang, H. Wang, Z. Qi, S. Liu, Strategy for In Situ Imaging of Cellular Alkaline Phosphatase Activity Using Gold Nanoflower Probe and Localized Surface Plasmon Resonance Technique, Analytical chemistry 90(23) (2018) 14056-14062.
[15] S.-S. Wang, X.-P. Zhao, F.-F. Liu, M.R. Younis, X.-H. Xia, C. Wang, Direct Plasmon-Enhanced Electrochemistry for Enabling Ultrasensitive and Label-Free Detection of Circulating Tumor Cells in Blood, Analytical chemistry 91(7) (2019) 4413-4420.
[16] F. López-Tejeira, R. Paniagua-Dominguez, J.A. Sánchez-Gil, High-performance nanosensors based on plasmonic Fano-like interference: probing refractive index with individual nanorice and nanobelts, ACS nano 6(10) (2012) 8989-8996.
[17] H. Aldewachi, T. Chalati, M. Woodroofe, N. Bricklebank, B. Sharrack, P. Gardiner, Gold nanoparticle-based colorimetric biosensors, Nanoscale 10(1) (2018) 18-33.
[18] H.J. Parab, C. Jung, J.-H. Lee, H.G. Park, A gold nanorod-based optical DNA biosensor for the diagnosis of pathogens, Biosensors and Bioelectronics 26(2) (2010) 667-673.

[19] M.-E. Yue, T.-F. Jiang, Y.-P. Shi, Determination of gallic acid and salidroside in Rhodiola and its preparation by capillary electrophoresis, Journal of Analytical Chemistry 61(4) (2006) 365-368.
[20] Ü.T. Yilmaz, A. Kekillioglu, R. Mert, Determination of Gallic acid by differential pulse polarography: Application to fruit juices, Journal of analytical chemistry 68(12) (2013) 1064-1069.
[21] J. Tashkhourian, S. Nami-Ana, A sensitive electrochemical sensor for determination of gallic acid based on SiO2 nanoparticle modified carbon paste electrode, Materials Science and Engineering: C 52 (2015) 103-110.
[22] F. Gao, D. Zheng, H. Tanaka, F. Zhan, X. Yuan, F. Gao, Q. Wang, An electrochemical sensor for gallic acid based on Fe2O3/electro-reduced graphene oxide composite: Estimation for the antioxidant capacity index of wines, Materials Science and Engineering: C 57 (2015) 279-287.
[23] R. Abdel-Hamid, E.F. Newair, Adsorptive stripping voltammetric determination of gallic acid using an electrochemical sensor based on polyepinephrine/glassy carbon electrode and its determination in black tea sample, Journal of Electroanalytical Chemistry 704 (2013) 32-37.
[24] B. Nikoobakht, M.A. El-Sayed, Preparation and growth mechanism of gold nanorods (NRs) using seed-mediated growth method, Chemistry of Materials 15(10) (2003) 1957-1962.
[25] C.J. Johnson, E. Dujardin, S.A. Davis, C.J. Murphy, S. Mann, Growth and form of gold nanorods prepared by seed-mediated, surfactant-directed synthesis, Journal of Materials Chemistry 12(6) (2002) 1765-1770.
[26] M. Friedman, H.S. Jürgens, Effect of pH on the stability of plant phenolic compounds, Journal of agricultural and food chemistry 48(6) (2000) 2101-2110.
[27] A.P. Leonov, J. Zheng, J.D. Clogston, S.T. Stern, A.K. Patri, A. Wei, Detoxification of gold nanorods by treatment with polystyrenesulfonate, ACS nano 2(12) (2008) 2481-2488.
[28] Y. Wang, D. Wan, S. Xie, X. Xia, C.Z. Huang, Y. Xia, Synthesis of silver octahedra with controlled sizes and optical properties via seed-mediated growth, ACS nano 7(5) (2013) 4586-4594.
[29] W. Wang, Q. Chen, C. Jiang, D. Yang, X. Liu, S. Xu, One-step synthesis of biocompatible gold nanoparticles using gallic acid in the presence of poly-(N-vinyl-2-pyrrolidone), Colloids and Surfaces A: Physicochemical and Engineering Aspects 301(1-3) (2007) 73-79.
[30] W. Niu, L. Zhang, G. Xu, Seed-mediated growth of noble metal nanocrystals: crystal growth and shape control, Nanoscale 5(8) (2013) 3172-3181.
[31] W. Shi, J. Casas, M. Venkataramasubramani, L. Tang, Synthesis and characterization of gold nanoparticles with plasmon absorbance wavelength tunable from visible to near infrared region, ISRN Nanomaterials 2012 (2012).
[32] J. Cao, T. Sun, K.T. Grattan, Gold nanorod-based localized surface plasmon resonance biosensors: A review, Sensors and actuators B: Chemical 195 (2014) 332-351.
[33] J.N. Anker, W.P. Hall, O. Lyandres, N.C. Shah, J. Zhao, R.P. Van Duyne, Biosensing with plasmonic nanosensors, Nanoscience and Technology: A Collection of Reviews from Nature Journals, World Scientific2010, pp. 308-319.
[34] C.J. Murphy, T.K. Sau, A.M. Gole, C.J. Orendorff, J. Gao, L. Gou, S.E. Hunyadi, T. Li, Anisotropic metal nanoparticles: synthesis, assembly, and optical applications, ACS Publications, 2005.
[35] J. Shen, B. Yan, M. Shi, H. Ma, N. Li, M. Ye, One step hydrothermal synthesis of TiO 2-reduced graphene oxide sheets, Journal of Materials Chemistry 21(10) (2011) 3415-3421.
[36] J. Zhang, H. Yang, G. Shen, P. Cheng, J. Zhang, S. Guo, Reduction of graphene oxide via L-ascorbic acid, Chemical Communications 46(7) (2010) 1112-1114.
[37] Y. Wang, Y. Zeng, W. Fu, P. Zhang, L. Li, C. Ye, L. Yu, X. Zhu, S. Zhao, Seed-mediated growth of Au@ Ag core-shell nanorods for the detection of ellagic acid in whitening cosmetics, Analytica chimica acta 1002 (2018) 97-104.

407

Table captions

Table 1. NRs size and surface charge measurement from TEM, DLS and zeta-potential anlyses

Table 2. Comparison of developed nanosensor with existing methods for gallic acid detection

Table 3. Analytical performance of GNRs for gallic acid detection

Table 4. Estimation of gallic acid in apple juice

Table 1. NRs size and surface charge measurement from TEM, DLS and zeta-potential anlyses

Samples	TEM				Mean hydrodynamic diameter (MHD) (nm)	Zeta potential (mV)
	Length (nm)	Breadth (nm)	AR	% spheres		
GNRs	63.01	21.76	2.89	2.01	80.3 ± 1.3	+42.12
GNRs + $HAuCl_4$ + 15 µM Gallic acid	61.16	25.66	2.38	3.02	82.1± 1.8	+41.33
GNRs + $HAuCl_4$ + 30 µM Gallic acid	60.22	29.89	2.01	3.68	86.3± 2.6	+37.82

Table 2. Comparison of developed nanosensor with existing methods for gallic acid detection

S. No.	Detection mode	Real sample	Linear range	LOD	Ref.
1	Capillary electrophoresis	Rhodiola root extract	24 –1200 µg/mL	2.4 µg/mL	[19]
2	Differential pulse polarograpghy	Fruit juice	1.0 – 50 µM	300 nM	[20]
3	SiO2 NPs based electrochemical sensor	Tea and orange juice	8.0×10^{-7} – 1.0×10^{-4} mol L^{-1}	250 nM	[21]
4	Fe_2O_3/electro-reduced graphene oxide composite based electrochemical sensor	Wine	1.0×10^{-6} M – 1.0×10^{-4} M	1.5×10^{-7} M	[22]
5	Polyepinephrin/glass carbon electrode	Black tea	1.0 – 20.0 µM	6.63×10^{-7} M	[23]
6	Thickness tunable GNRs	Apple juice	1.25 – 20 µM	90 nM	Our work

Table 3 Analytical performance of GNRs for gallic acid detection

Analyte	Linear regression equation	R^2	LOD (nM)	RSD		
				Run-to-Run	Day-to-Day	Batch-to-Batch
Gallic acid	y = 2.6279x + 1.9159	0.99	90	1.14	1.18	2.32

Table 4. Estimation of gallic acid in apple juice

Sample	Concentration of gallic acid (µM)		% Recovery	% RSD (n=3)
	Added	Found		
Apple juice	5	4.97	99.46	1.50
	10	10.04	100.46	4.36
	20	20.68	103.4	0.62

Research Highlights

- Sensitive and selective detection of gallic caid
- Tuning the aspect ratio of Gold Nanorods in presence of gallic acid
- Blue-shift of the LSPR in presence of anti-oxidant
- Low detection limt and good recovery in real food sample

Conflict of Interests statement

The authors have no conflicts of interest to declare.